Integration of the Manzanares Solar Chimney Power Plants in Towers: Collector and Building Height Configuration

Meriem Hafidha Titi
Laboratory of Architecture, Urbanism and Transport (LAUTR), Institute of Architecture and Urbanism, University of Batna 1, Algeria
meriemhafidha.titi@univ-batna.dz

Ammar Mebarki
Institute of Architecture and Urbanism, University of Batna 1, Algeria
ammar.mebarki@univ-batna.dz (corresponding author)

Abdelhalim Assassi
Institute of Architecture and Urbanism, University of Batna 1, Algeria | Laboratory of Habitat and Environnement (LHE), University of Setif 1, Algeria
abdelhalim.assassi@univ-batna.dz

Received: 16 February 2025 | Revised: 28 February 2025 and 17 March 2025 | Accepted: 23 March 2025

 DOI: https://doi.org/10.48084/etasr.10594

ABSTRACT

Solar Chimney Power Plants (SCPP) are renewable electricity production systems that use greenhouse and wind turbine technologies. Due to their large dimensions, they are only installed in rural areas. A few studies have addressed the use of SCPP in urban areas, as independent systems. This research aims to integrate the chimneys into high-rise buildings, utilizing the roof as a solar collector, in order to minimize the necessary land area. The impact of building height and collector configuration on the system outputs were investigated using 3D Computational Fluid Dynamics (CFD) and Ansys fluent analysis. The results reveal that the highest total energy production can be achieved by installing the turbines both at the top and bottom of the chimney, on a building of 140 m height. In this setting the energy production is 6.62 kW at the top and 26.81 kW at the bottom, resulting in a total of 33.47 kW. This study highlights the effectiveness of the proposed strategy in energy generation systems in high-rise buildings.

Keywords-SCPP integration; CFD simulation; energy generation; high-rise building

I. INTRODUCTION

The concept of energy transition involves a shift from traditional fossil fuels to the production of electricity, heat, and mechanical energy through renewable energy [1]. SCPP are renewable energy systems that convert solar energy into electricity, using a combination of greenhouse, chimney, and wind turbine technologies [2–5]. These plants consist of a solar collector, an updraft tower, and turbines, which generate power from the buoyant air flow created by solar heating. Large-scale plants could potentially replace fossil fuel-based power generation [6, 7]. The first appearance of the SCPP was in Manzanares, Spain in 1982 [8-11]. CFD technologies open up new opportunities for the development of power engineering [12, 13]. Many researchers have extensively used the CFD models to investigate various aspects of the plant's performance, including the effects of chimney height, solar radiation, and atmospheric temperature [14, 15]. Authors in [16] found that increasing the height of the chimney leads to exponential growth in air velocity and mass flow rate, while reducing the temperature in the collector. An analysis of the solar chimney's overall efficiency revealed a direct relationship with chimney height. It was found that the large-scale up to 1000 m could produce about 400 MW and could continuously generate power, even during the night, due to ground thermal capacity [17, 18]. Optimizing collector shape and height could increase the annual power output [8, 17, 19, 20]. It is known that SCPP is used only in rural areas, as the system is large in size and is not compatible with urban areas. Recent research has been focused on adapting SCPPs for urban environments by scaling down their dimensions, proposing equations that demonstrate the relation between scale decrease and air velocity, pressure difference, mass flow rate, and generated energy [21]. Authors in [22] proposed a novel vertical SCPP design for building integration that improved its performance compared to conventional systems, with the power output

being affected by several factors, such as chimney height and diameter. The impact of collector angle (from 360° to 120°) on energy outputs in high-rise buildings has also been studied [23]. Indeed, the multidisciplinary collaboration encompassing architecture, thermal physics, aerodynamics, materials science, and biology seem to be necessary for the successful implementation of this system in urban areas [24]. It is worth noting that previous studies have dealt with the SCPP system in urban areas as independent constructions, without incorporating it in the building components. Therefore, this research aims to integrate the SCPP inside high-rise buildings by using a vertical height cavity as a chimney and employing the roof area as a collector in order to minimize the use of the surrounding area. In addition, the current paper studied the impact of building height and collector configuration on system outputs including air velocity, air temperature, pressure difference, and power generation.

II. PHYSICAL MODEL

This study is based on the Manzanares SCPP model, with 194.6 m, 10.16 m, 122 m, and 1.85 m corresponding to chimney height, chimney diameter, collector radius, and collector height, respectively [25, 26]. The turbine is positioned at the bottom of the chimney, above the collector level. Additionally, the ground beneath the collector serves as a thermal storage medium, contributing to energy retention and heat distribution.

III. NUMERICAL MODEL

CFD simulations were performed using Ansys Fluent analysis, applying the k-ε turbulence model and Boussinesq approximation [27, 28]. Authors in [29, 30] focused on airflow, solar radiation, and thermal storage, with optimized collector designs proposed for improved efficiency.

- The equation of continuity:

$$\frac{\partial \rho}{\partial t} + \frac{1}{r}\frac{\partial (\rho u r)}{\partial r} + \frac{\partial (v r)}{\partial z} = 0 \quad (1)$$

$$\frac{\partial (pu)}{\partial t} + \frac{1}{r}\frac{\partial}{\partial r}(pruu) + \frac{\partial (\rho uv)}{\partial z} = -\frac{\partial p}{\partial r} + \frac{1}{r}\frac{\partial}{\partial r}\left(\mu r \frac{\partial u}{\partial r}\right) + \frac{\partial}{\partial z}\left(\mu \frac{\partial u}{\partial z}\right) - 2\mu \frac{u}{r^2} \quad (2)$$

$$\frac{\partial (\rho v)}{\partial t} + \frac{1}{r}\frac{\partial}{\partial r}(\rho ruv) + \frac{\partial (\rho \vartheta v)}{\partial z} = -\frac{\partial \rho}{\partial z} + \frac{1}{r}\frac{\partial}{\partial r}\left(\mu r \frac{\partial \vartheta}{\partial r}\right) + \frac{\partial}{\partial z}\left(\mu \frac{\partial \vartheta}{\partial z}\right) - (\rho_0 - \rho)g \quad (3)$$

$$\frac{\partial (\rho C_p T)}{\partial t} + \frac{1}{r}\frac{\partial}{\partial r}\left(\rho r C_p u T\right) + \frac{\partial (\rho C_p v T)}{\partial z} = \frac{1}{r}\frac{\partial}{\partial r}\left(r\lambda \frac{\partial T}{\partial r}\right) + \frac{\partial}{\partial z}\left(\lambda \frac{\partial T}{\partial z}\right) - \nabla . q_r \quad (4)$$

- The Rayleigh number (*Ra*) measures the buoyancy-induced flow strength in the natural convection:

$$R_a = \frac{g\beta \Delta T L^3}{av} \quad (5)$$

where ΔT is the maximum temperature difference of the system, β is the thermal expansion coefficient, L is the mean collector height, and a is the thermal diffusivity .

- The Reynolds number (*Re*) exceeds 10^{10}, suggesting the potential for turbulent fluid [31, 32]. The RNG k-ε model was employed to simulate this turbulent flow [33]. The turbulent kinetic energy k, and its dissipation rate ε, were derived from the two transport equations [34]:

$$\frac{\partial (\rho k)}{\partial t} + \frac{\partial}{\partial X_i}(\rho K u_i) = \frac{\partial}{\partial X_j}\left(\alpha_k \mu_{eff} \frac{\partial K}{\partial X_j}\right) + G_K + G_b - \rho\varepsilon - Y_M \quad (6)$$

$$\frac{\partial (\rho \varepsilon)}{\partial t} + \frac{\partial}{\partial X_j}(\rho \varepsilon u_i) = \frac{\partial}{\partial X_j}\left(\alpha_\varepsilon \mu_{eff} \frac{\partial \varepsilon}{\partial X_j}\right) + G_{1\varepsilon}\frac{\varepsilon}{k}(G_k + G_{3\varepsilon}G_b) - G_{2\varepsilon}\rho\frac{\varepsilon^2}{k} - R_\varepsilon \quad (7)$$

where:

G_k: Generation of turbulent kinetic energy having resulted from the mean velocity gradients

G_b: Generation of turbulent kinetic energy having resulted from buoyancy

σ_T = 0.9, σ_k = 1.0, σ_ε= 1.3 are the *T*, *k*, and ε turbulent Pranldt numbers, respectively.

$G_{1\varepsilon}$= 1.44, $G_{2\varepsilon}$ = 1.92, and C_μ = 0.09 are the constants for the turbulent model.

- The Turbine:

The turbines convert the kinetic energy of air into mechanical energy and finally to electrical energy [35, 36].

The rotor gets the following mechanical power:

$$P_m = \frac{2}{3}\eta_{col}\eta_{ch}A_{col}G \quad (8)$$

The equation above can be further detailed as:

$$P_m = \frac{2}{3}\eta_{col}\eta_{ch}\pi r^2 G \quad (9)$$

IV. CONFIGURATION

In order to better study innovation, several proposals were examined, and the three most important models are presented in this section. In residential buildings with four apartments of 135 m^2 on each floor, the average of global superficies, including circulation and chimney cavity (diameter of 10.18 m), is 800 m^2 (building radius = 16 m).

First model: The roof of the building serves as ground, on top of which a collector with a radius of 11 m is placed. An air inlet is provided at the bottom of the building, as depicted in Figure 1(a).

Second model: Similar to the first model, with the addition of one more collector around the building, covering the same area as the collector on the roof. In this case there is also only one inlet at the bottom of the building, as portrayed in Figure 1(b).

Third model: Similar to the second model, with the addition of an air inlet at the upper collector, as shown in Figure 1(c).

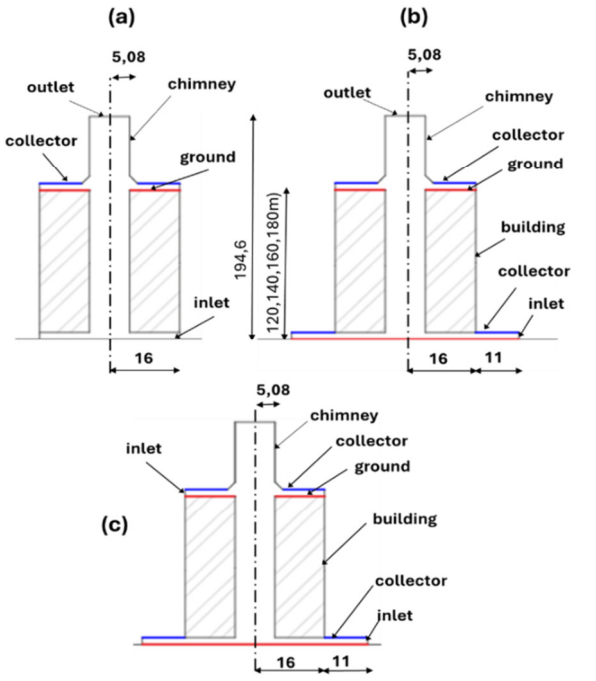

Fig. 1. Solar chimney power plant configuration: (a) first model, (b) second model, (c) third model.

V. BOUNDARY CONDITIONS

The Ansys Fluent is used to simulate all models, by implementing three-dimensional axial CFD for 15° parts of the proposed models to accelerate convergence. This study used the RNG k-ε turbulence model, the SIMPLE algorithm, and PRESTO method to solve the momentum equations, and determine the relationship between pressure, air velocity, and pressure interpolation, respectively. The non-grey radiation (DO) in conjunction with the solar ray tracing technique was adopted for radiation calculations. To clarify the relationship between temperature and variations in air density, the Boussinesq approximation was activated. The material properties adopted are presented in Figure 1 and in Table I.

TABLE I. MATERIAL PROPERIES OF SCPP ADOPTED IN THIS STUDY

	Chimney	**Glass**	**Ground**
Thickness (m)	0.00125	0.004	0.5
Density (kg/m^3)	8030	2500	2160
Thermal conductivity (W/mK)	16.27	1.15	1.83
Specific heat (J/kgK)	502.48	750	710
Absorption coefficient	0	0.03	0.9
Transmissivity	-	0.9	-
Emissivity	1	0.9	0.9
Reflective index	1	1.526	1

Conditions: Air Temperature of 293.15 K

VI. RESULTS AND DISCUSSION

Figure 2 illustrates the CFD simulation results of the air velocity and temperature for the three models at the outlet of the collector at the bottom of the building. The three tested models recorded air velocity of 11.1, 9.07, and 8.23 m/s and a temperature difference of 3.85, 6.85, and 7.35 k, respectively, as evidenced in Figure 3.

The addition of the lower collector increased the temperature between models 1 and 2 by 3 K. On the other hand, the horizontal dimension of this collector reduced the air velocity at the bottom of the chimney by 2.03 m/s.

The addition of the air inlet in the upper collector raised the temperature inside the chimney tunnel by 0.5 K, while the effect of the air movement momentum at the upper collector level reduced the air velocity by 0.84 m/s at the bottom of the chimney between models 2 and 3.

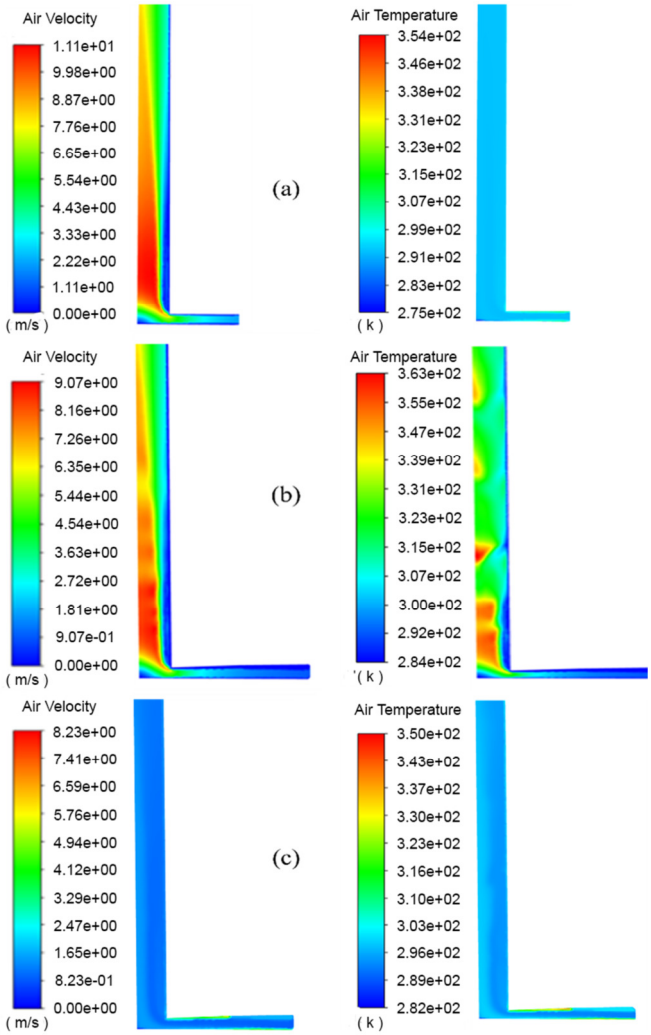

Fig. 2. CFD simulation results of air velocity and temperature at the outlet of the collector at the bottom of the building: (a) first model, (b) second model, (c) third model.

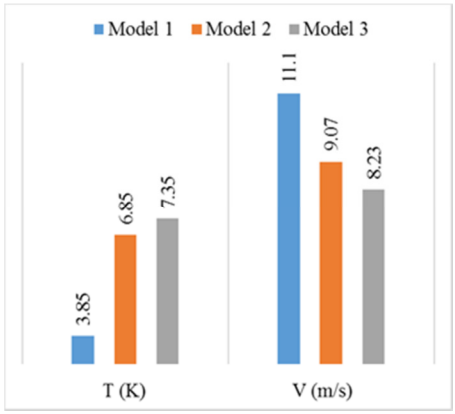

Fig. 3. The values of air velocity and air temperature difference at the outlet of the collector at the bottom of the building of the three models.

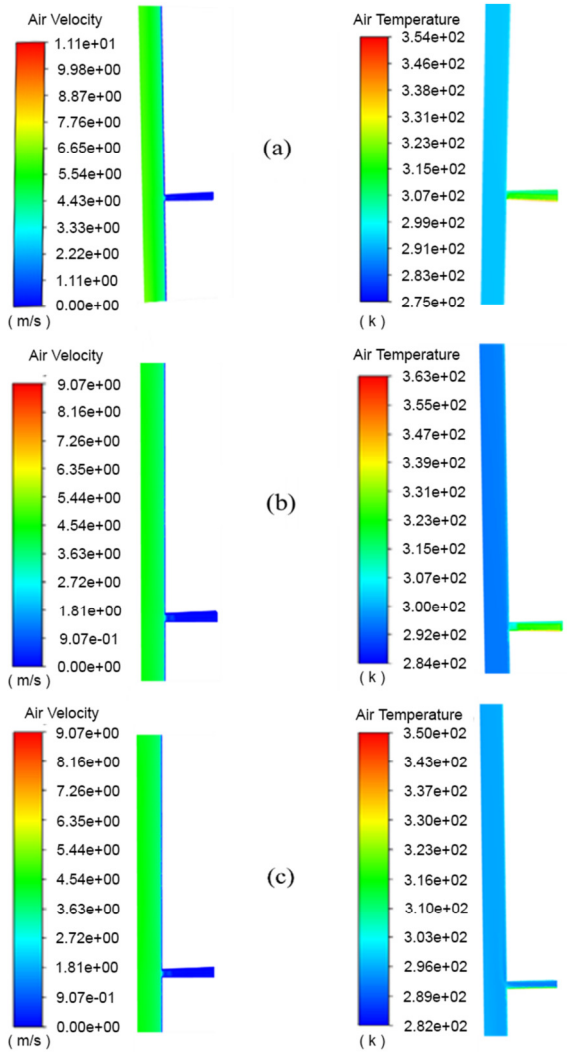

Fig. 4. CFD Simulation results of air velocity and air temperature difference at the upper collector level: (a) first model, (b) second model, (c) third model

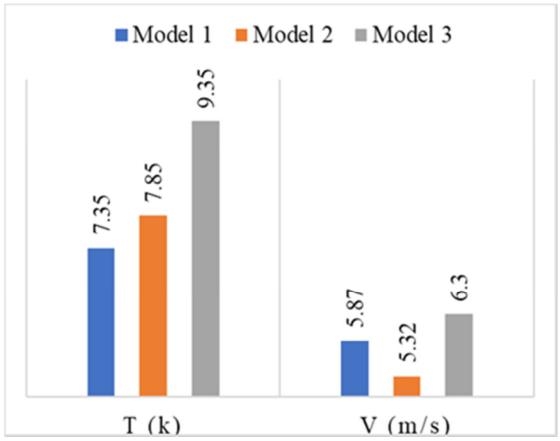

Fig. 5. The values of air velocity and air temperature difference at the upper collector level of the three models.

The CFD simulation results of the air velocity and air temperature difference at the upper collector level are presented in Figure 4. Air velocity recorded 5.87, 5.32, and 6.3 m/s, with temperature differences of 7.35, 7.85, and 9.35 K for the three models, respectively.

The addition of the lower collector increased the temperature between models 1 and 2 by 0.5 K. The decrease in the air velocity at the top of the building by 0.55 m/s is affected by the decrease in air velocity in the entire chimney tunnel. The new inlet in the upper collector increased the temperature by 1.5 K and the air velocity by 0.98 m/s, which is affected by the complete thermal participation of the upper collector.

Table II illustrates the energy generated at the upper and lower collectors of the three models, as well as the global energy. The implementation of the third model can generate more energy than the other two, so the rest of the study will be based on it.

TABLE II. THE GENERATED ENERGY AT THE UPPER AND THE LOWER COLLECTORS FOR THE THREE MODELS

	Model 1	**Model 2**	**Model 3**
Energy (upper collector)	14.42 kW	20.94 kW	20.39 kW
Energy (lower collector)	5.574 kW	5.395 kW	7.610 kW
Energy (global)	20 kW	26.33kW	28 kW

VII. IMPACT OF BUILDING HEIGHT ON PROPOSED SYSTEM OUTPUTS

To study the effect of building height, while maintaining the total height of the chimney 194.6 m, four heights, namely 120, 140, 160, and 180 m were tested for the third model, selected from the previous part of this study (a model equipped with two collectors, and an air inlet for each collector).

Figure 6 shows that the increase of the building height increases the air velocity at the lower turbine, affected by the increased distance of the momentum point of the upper collector, according to the following polynomial equation:

$$y = -0.0014x^2 + 0.5483x - 37.028 \quad (10)$$

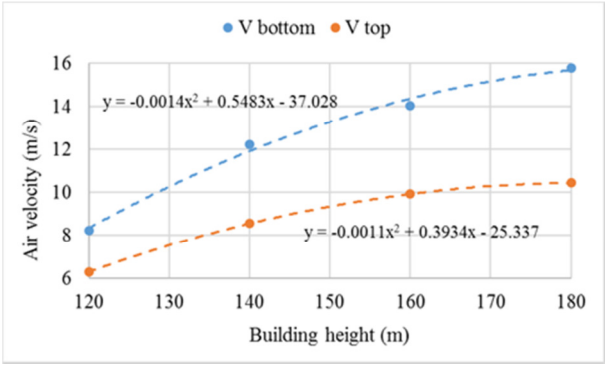

Fig. 6. The effect of building height on air velocity for the lower and the upper collectors.

The air velocity at the level of the upper turbine also increases, with slower rate, affected by the increase in the air velocity in the chimney tunnel, according to:

$$y = -0.0011x^2 + 0.3934x - 25.337 \quad (11)$$

Figure 7 displays the decrease in air temperature difference at the lower and upper turbines, affected by the air velocity rise, which accelerates the drain of hot air, according to:

$$y = -7E-05x^2 - 0.0316x + 14.103 \quad (12)$$

$$y = 0.0003x^2 - 0.1248x + 17.825 \quad (13)$$

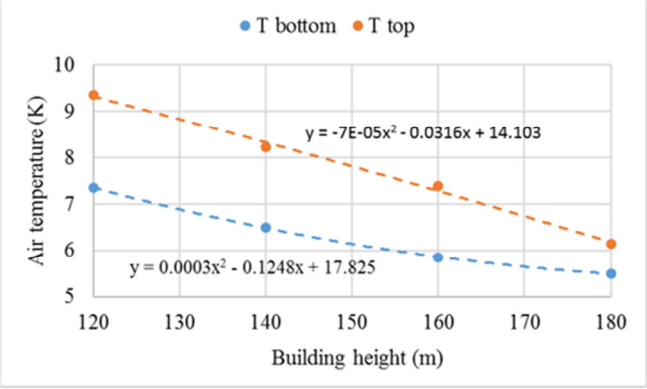

Fig. 7. The effect of building height on air temperature difference for the lower and the upper collectors.

The generated energy at the lower and the upper turbine levels, in addition to the global energy are presented in Figure 8, which shows that the energy produced in the lower turbine increases with the building height according to an increasing polynomial:

$$y = -0.003x^2 + 1.0489x - 61.447 \quad (14)$$

while the produced energy in the upper turbine decreases with the building height according to a decreasing polynomial:

$$y = -0.0011x^2 + 0.239x - 4.699 \quad (15)$$

The total energy versus building height graph shows that energy production reaches its peak at 140 m, producing 33.47 kW, then it begins to decrease according to:

$$y = -0.0042x^2 + 1.2879x - 66.145 \quad (16)\backslash$$

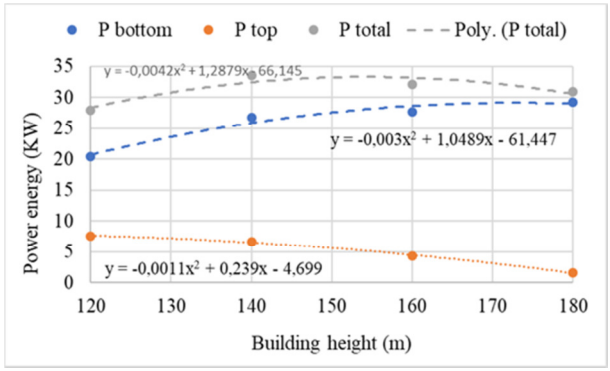

Fig. 8. The effect of building height on the generated energy at the lower collector, the upper collector, and the total energy.

VIII. CONCLUSION

The Solar Chimney Power Plants (SCPP) system is used only in rural areas as its large size is not compatible with urban areas. Previous studies have researched the potential of introducing SCPP systems in urban areas as independent structures. The present paper proposed the incorporation of SCPP within high-rise buildings, aiming to integrate them in the urban setting. After testing three models in the first stage, a model equipped with two solar collectors (bottom and top of the building) was selected, where a limited area of the building's surrounding land was used. The height of the building was utilized as a cavity for the chimney. In the second stage, the research focused on the effect of the building height on the system outputs, using polynomial equations for air temperature, air velocity, and energy. The results indicated that a system with a top and a bottom turbine, on a building of 140 m height can achieve the maximum energy production of 33.47 kW. In this setting, the bottom turbine produces 26.81 kW and the top turbine 6.62 kW. This study suggests that SCPP systems could be an effective energy generation method for high-rise buildings.

ACKNOWLEDGMENT

This study was supported by Directorate General for Scientific Research and Technological Development (DGRSDT) of the Algerian Ministry of Higher Education and Scientific Research.

RESEARCH PROJECT: A02L01UN050120230001.

REFERENCES

[1] N. Cruz-Pérez *et al.*, "SWOT Analysis of the Benefits of Hydropower Energy in Four Archipelagos," *Civil Engineering Journal*, vol. 10, no. 7, pp. 2370–2383, Jul. 2024, https://doi.org/10.28991/CEJ-2024-010-07-019.

[2] R. Bais and N. Saxena, "A Review on Solar Chimney Power Plant Performance," *International Journal for Research Trends and Innovation*, vol. 6, no. 2, pp. 32-27, Feb. 2021.

[3] X. Zhou, T. W. Von Backström, and M. A. D. S. Bernardes, "Introduction to the Special Issue on Solar Chimneys," *Solar Energy*, vol. 98, pp. 1, Dec. 2013, https://doi.org/10.1016/j.solener.2013.10.029.

[4] M. O. Hamdan, "Analysis of a solar chimney power plant in the Arabian Gulf region," *Renewable Energy*, vol. 36, no. 10, pp. 2593–2598, Oct. 2011, https://doi.org/10.1016/j.renene.2010.05.002.

[5] B. K. Behera, S. S. Sahoo, and S. Kumar, "Technology, design, and performance of solar chimney power plants: An updated and thorough review," *International Journal of Green Energy*, pp. 1–34, Dec. 2024, https://doi.org/10.1080/15435075.2024.2446492.

[6] P. Belkhode, C. Sakhale, and A. Bejalwar, "Evaluation of the experimental data to determine the performance of a solar chimney power plant," *Materials Today: Proceedings*, vol. 27, pp. 102–106, 2020, https://doi.org/10.1016/j.matpr.2019.09.006.

[7] M. Bayareh, "Exergy analysis of solar chimney power plants: A review," *Sustainable Energy Technologies and Assessments*, vol. 53, Oct. 2022, Art. no. 102568, https://doi.org/10.1016/j.seta.2022.102568.

[8] W. Haaf, K. Friedrich, G. Mayr, and J. Schlaich, "Solar Chimneys Part I: Principle and Construction of the Pilot Plant in Manzanares," *International Journal of Solar Energy*, vol. 2, no. 1, pp. 3–20, Jan. 1983, https://doi.org/10.1080/01425918308909911.

[9] W. Haaf, "Solar Chimneys: Part II: Preliminary Test Results from the Manzanares Pilot Plant," *International Journal of Solar Energy*, vol. 2, no. 2, pp. 141–161, Jan. 1984, https://doi.org/10.1080/01425918408909921.

[10] J. Schlaich, R. Bergermann, W. Schiel, and G. Weinrebe, "Design of Commercial Solar Updraft Tower Systems—Utilization of Solar Induced Convective Flows for Power Generation," *Journal of Solar Energy Engineering*, vol. 127, no. 1, pp. 117–124, Feb. 2005, https://doi.org/10.1115/1.1823493.

[11] P. Das and C. Velayudhan Parvathy, "A critical review on solar chimney power plant technology: influence of environment and geometrical parameters, barriers for commercialization, opportunities, and carbon emission mitigation," *Environmental Science and Pollution Research*, vol. 29, no. 46, pp. 69367–69387, Oct. 2022, https://doi.org/10.1007/s11356-022-22623-7.

[12] Y. A. Sazonov, M. A. Mokhov, A. V. Bondarenko, V. V. Voronova, K. A. Tumanyan, and E. I. Konyushkov, "Study of Reversible Nozzle Apparatuses Using Euler Methodology and CFD Technologies," *Civil Engineering Journal*, vol. 10, no. 11, pp. 3640–3671, Nov. 2024, https://doi.org/10.28991/CEJ-2024-010-11-013.

[13] M. Sukkee and P. Kongphan, "Innovative Metal Powder Production Using CFD with Convergent-Divergent Nozzles in Wire Arc Atomization," *HighTech and Innovation Journal*, vol. 5, no. 3, pp. 551–571, Sep. 2024, https://doi.org/10.28991/HIJ-2024-05-03-02.

[14] U. E. Ayli, E. Özgirgin, and M. Tareq, "Solar Chimney Power Plant Performance for Different Seasons Under Varying Solar Irradiance and Temperature Distribution," *Journal of Energy Resources Technology*, vol. 143, no. 6, Jun. 2021, Art. no. 061303, https://doi.org/10.1115/1.4048533.

[15] E. Cuce, P. M. Cuce, and H. Sen, "A thorough performance assessment of solar chimney power plants: Case study for Manzanares," *Cleaner Engineering and Technology*, vol. 1, Dec. 2020, Art. no. 100026, https://doi.org/10.1016/j.clet.2020.100026.

[16] E. Cuce, H. Sen, and P. M. Cuce, "Numerical performance modelling of solar chimney power plants: Influence of chimney height for a pilot plant in Manzanares, Spain," *Sustainable Energy Technologies and Assessments*, vol. 39, Jun. 2020, Art. no. 100704, https://doi.org/10.1016/j.seta.2020.100704.

[17] L. B. Mullett, "The solar chimney—overall efficiency, design and performance," *International Journal of Ambient Energy*, vol. 8, no. 1, pp. 35–40, Jan. 1987, https://doi.org/10.1080/01430750.1987.9675512.

[18] A. B. Kasaeian, Sh. Molana, K. Rahmani, and D. Wen, "A review on solar chimney systems," *Renewable and Sustainable Energy Reviews*, vol. 67, pp. 954–987, Jan. 2017, https://doi.org/10.1016/j.rser.2016.09.081.

[19] D. Kröger and J. Buys, "Performance Evaluation of a Solar Chimney Power Plant," 2001, [Online]. Available: https://www.semanticscholar.org/paper/Performance-Evaluation-of-a-Solar-Chimney-Power-Kr%C3%B6ger-Buys/203c732bc341203e165310e6108f43ff3fe1b08b.

[20] R. Sangi, "Performance evaluation of solar chimney power plants in Iran," *Renewable and Sustainable Energy Reviews*, vol. 16, no. 1, pp. 704–710, Jan. 2012, https://doi.org/10.1016/j.rser.2011.08.035.

[21] A. Mebarki, A. Sekhri, A. Assassi, A. Hanafi, and B. Marir, "CFD analysis of solar chimney power plant: Finding a relationship between model minimization and its performance for use in urban areas," *Energy Reports*, vol. 8, pp. 500–513, Nov. 2022, https://doi.org/10.1016/j.egyr.2021.12.008.

[22] S. Bagheri and M. Ghodsi Hassanabad, "Numerical and experimental investigation of a novel vertical solar chimney power plant for renewable energy production in urban areas," *Sustainable Cities and Society*, vol. 96, Sep. 2023, Art. no. 104700, https://doi.org/10.1016/j.scs.2023.104700.

[23] M. Saad, N. Ahmed, L. Giovannini, M. Mahmood, M. U. Rafi, and M. A. Qaisrani, "Evaluation of possible integration of solar chimney power plants with high-rise buildings: A numerical analysis," *Journal of Building Engineering*, vol. 60, Nov. 2022, Art. no. 105188, https://doi.org/10.1016/j.jobe.2022.105188.

[24] B. Wang and Z. Wang, "High-rise Building Integrated with Solar Chimney and Bioenergy," *IOP Conference Series: Earth and Environmental Science*, vol. 898, no. 1, Oct. 2021, Art. no. 012028, https://doi.org/10.1088/1755-1315/898/1/012028.

[25] S. Ali and B. Djaouida, "Investigating the Feasibility of Integrating Vegetation into Solar Chimney Power Plants in the Tamanrasset Region," *Engineering, Technology & Applied Science Research*, vol. 14, no. 3, pp. 14719–14724, Jun. 2024, https://doi.org/10.48084/etasr.7506.

[26] H. Şen, A. P. M. Cüce, and E. Cüce, "Impacts of Collector Radius and Height on Performance Parameters of Solar Chimney Power Plants: A Case Study for Manzanares, Spain," *Recep Tayyip Erdogan University Journal of Science and Engineering*, vol. 2, no. 2, pp. 83–104, Dec. 2021, https://doi.org/10.53501/rteufemud.1017909.

[27] R. Rabehi, A. Chaker, Z. Aouachria, and M. Tingzhen, "CFD analysis on the performance of a solar chimney power plant system: Case study in Algeria," *International Journal of Green Energy*, vol. 14, no. 12, pp. 971–982, Sep. 2017, https://doi.org/10.1080/15435075.2017.1339043.

[28] A. Ayadi, Z. Driss, and M. S. Abid, "Experimental and computational analysis of the collector geometry of a solar chimney," *Environmental Progress & Sustainable Energy*, vol. 38, no. 6, 2019, Art. no. e13238, https://doi.org/10.1002/ep.13238.

[29] M. Senbeto, "Numerical Simulations of Solar Chimney Power Plant with Thermal Storage," *International Journal of Engineering Research and Technology*, vol. 9, no. 10, Oct. 2020.

[30] R. Laouar and O. Wuensch, "Numerical investigation on the performance of a Solar Chimney Power Plant System (SCPP)," *PAMM*, vol. 23, no. 1, 2023, Art. no. e202200320, https://doi.org/10.1002/pamm.202200320.

[31] Md. S. Hossain, Md. I. Hossain, S. Pramanik, and Dr. J. U. Ahamed, "Analyzing the Turbulent Flow Characteristics by Utilizing k-ϵ Turbulence Model.," *European Journal of Engineering Research and Science*, vol. 2, no. 11, pp. 28, Nov. 2017.

[32] P. Caicedo, D. Wood, and C. Johansen, "Radial Turbine Design for Solar Chimney Power Plants," *Energies*, vol. 14, no. 3, Jan. 2021, Art. no. 674, https://doi.org/10.3390/en14030674.

[33] G. G. R. Gunadi, A. I. Siswantara, Budiarso, A. Daryus, and H. Pujowidodo, "Study of turbulence models application in crossflow turbine analysis," *AIP Conference Proceedings*, vol. 2062, no. 1, Jan. 2019, Art. no. 020014, https://doi.org/10.1063/1.5086561.

[34] G. Wang *et al.*, "Estimation of the dissipation rate of turbulent kinetic energy: A review," *Chemical Engineering Science*, vol. 229, Jan. 2021, Art. no. 116133, https://doi.org/10.1016/j.ces.2020.116133.

[35] E. Kulunk, "Aerodynamics of Wind Turbines," in *Fundamental and Advanced Topics in Wind Power*, IntechOpen, 2011.

[36] I. H. Al-Bahadly, *Wind Turbines*. BoD – Books on Demand, 2011.